Supplementary Information

One-step synthesized Nb_2O_{5-y}-decorated spinel-type $(Ni,V,Mn)_3O_{4-x}$ nanoflowers for boosting electrocatalytic reduction of nitrogen into ammonia

Tadele Negash Gemeda[1], Dong-Hau Kuo[1,2*], Quoc-Nam Ha[1]

[1] Department of Materials Science and Engineering, National Taiwan University of Science and Technology, No. 43, Sec. 4, Keelung Road, Taipei 10607, Taiwan.

[2] Graduate Institute of Energy and Sustainability Technology, National Taiwan University of Science and Technology, No. 43, Sec. 4, Keelung Road, Taipei 10607, Taiwan.

*Corresponding author

Fax: +011-886-2-27303291. E-mail: dhkuo@mail.ntust.edu.tw

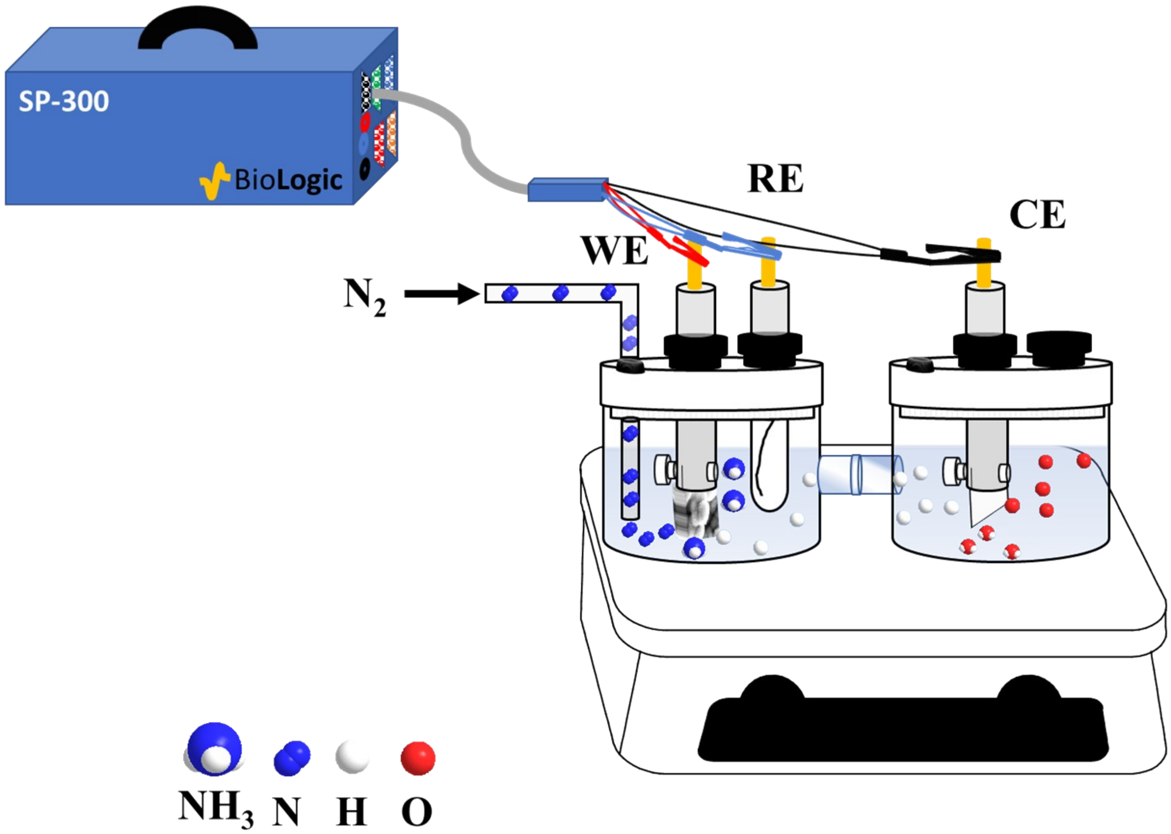

Fig. S1. H-cell compartment setup for electrochemical analysis.

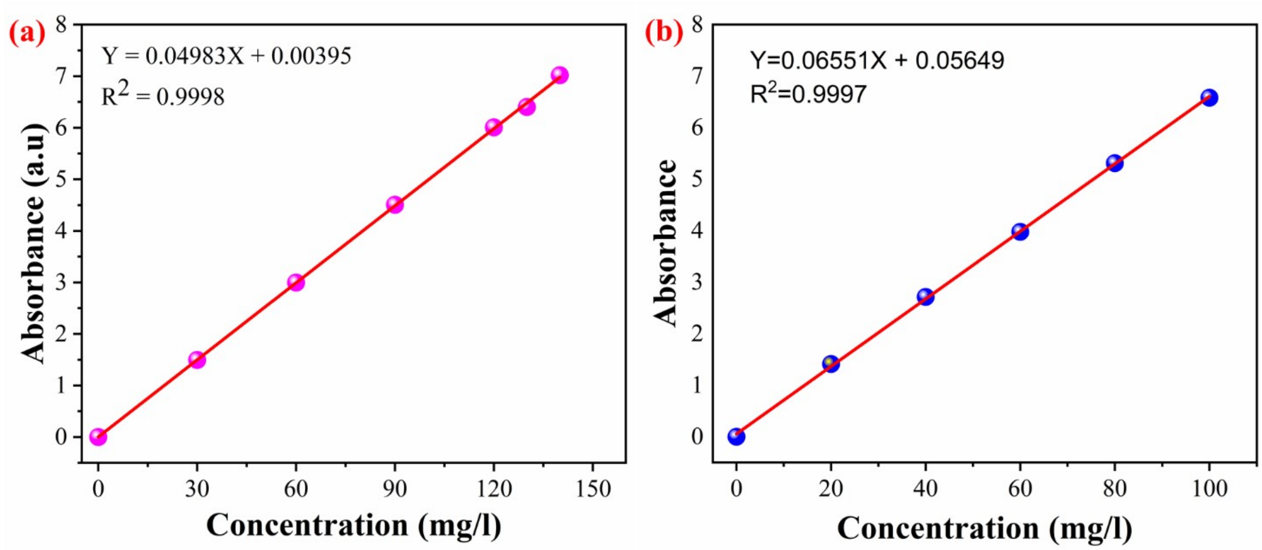

Fig. S2. UV-Vis calibration for (a) NH_3 detection and (b) N_2H_4 detection.

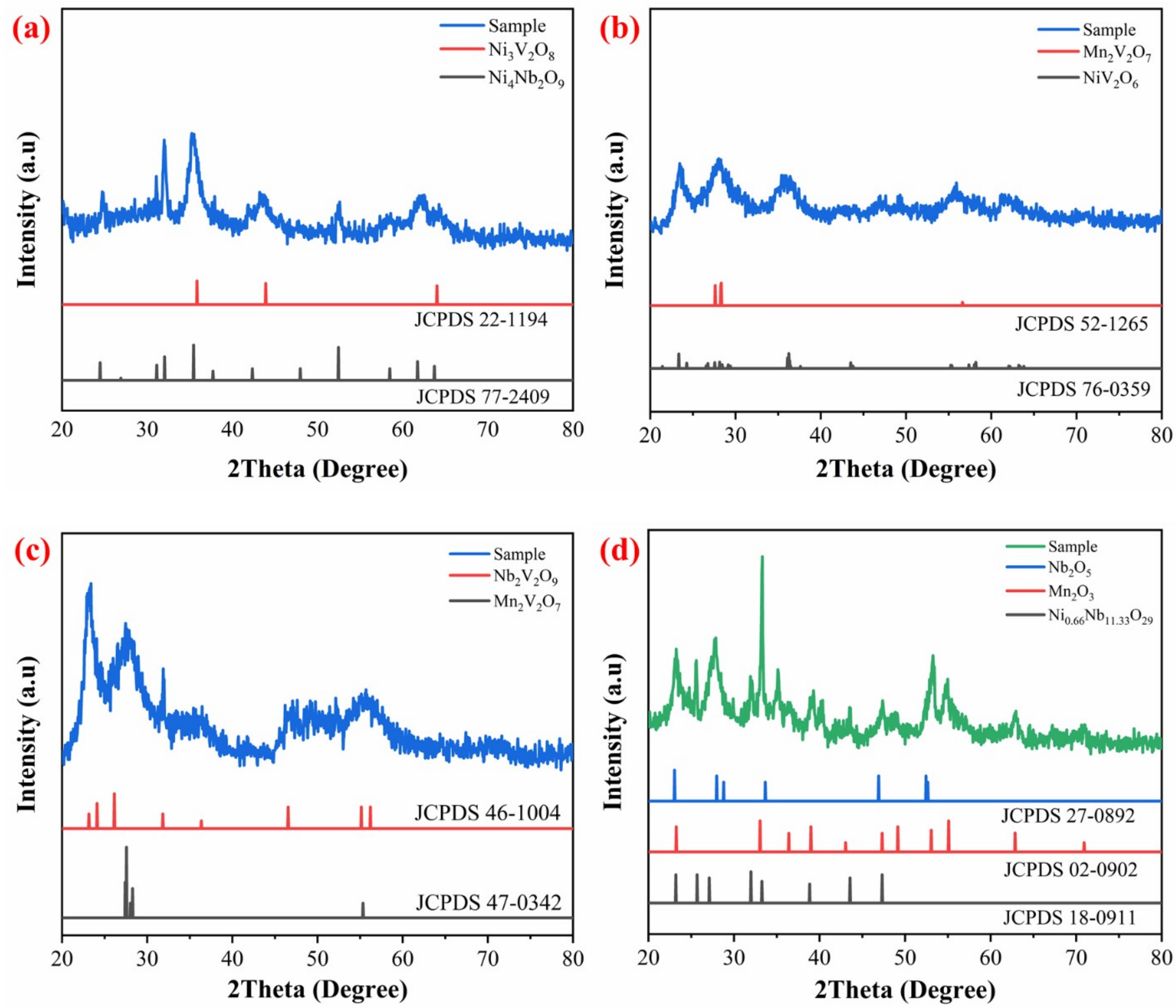

Fig. S3. X-ray diffraction (XRD) pattern for ternary metal-oxide system (a) NiVNb-666, b) NiVMn-662, c) VMnNb-626, and d) NiMnNb-626.

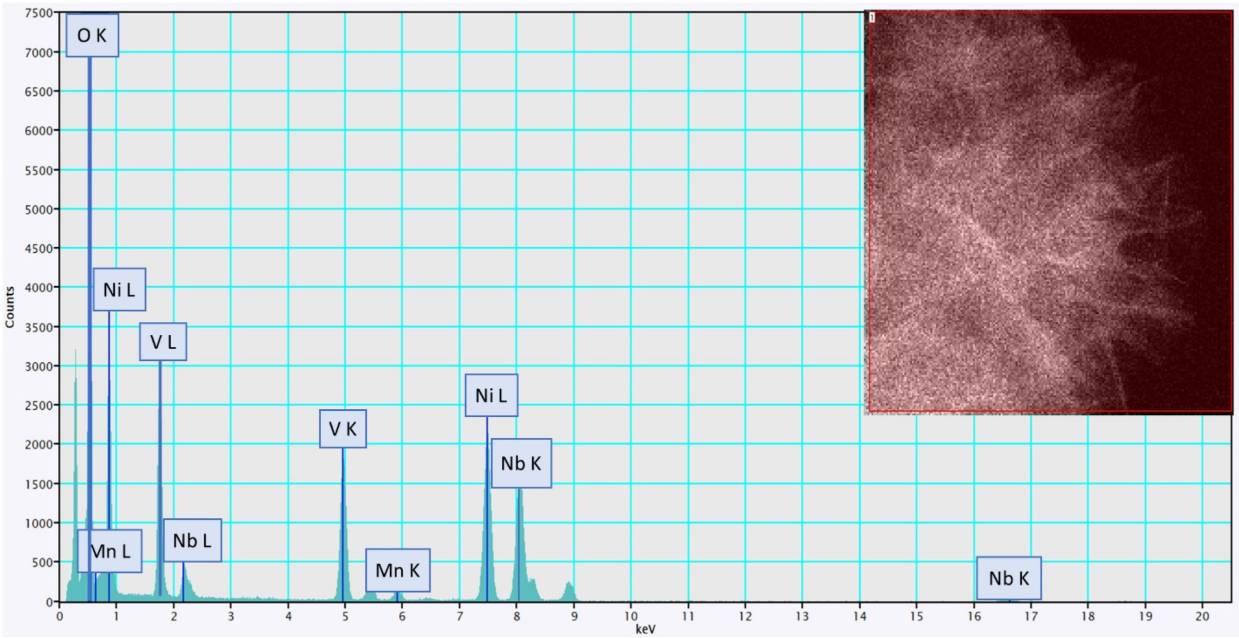

Fig. S4. STEM-EDS images of spinel-type $(Ni,V,Mn)_3O_{4-x}/Nb_2O_{5-y}$ nanoflowers on nickel foam.

.

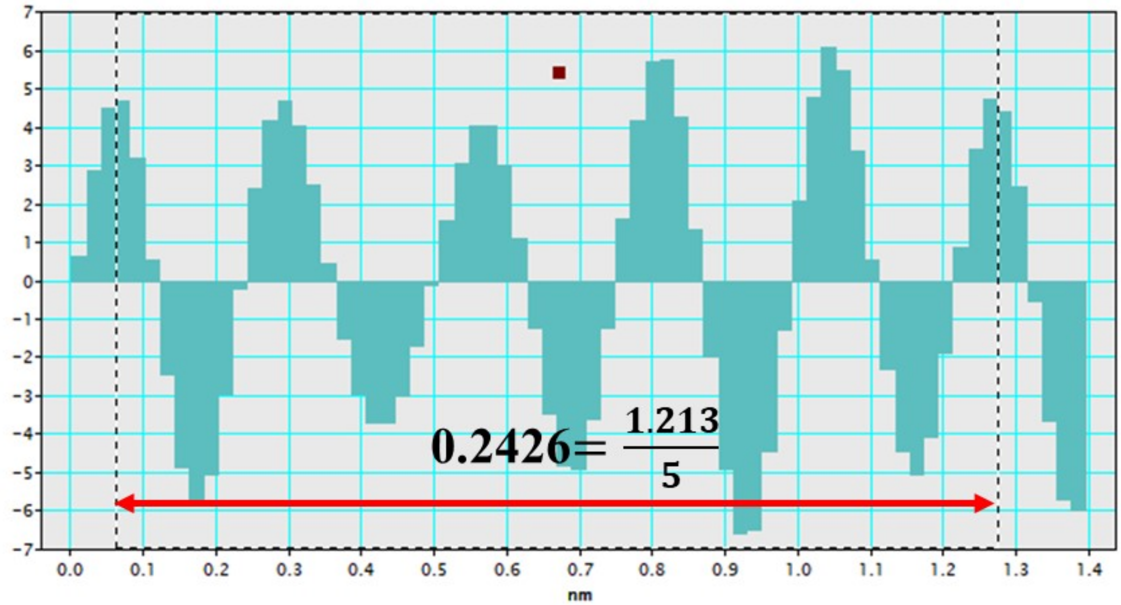

Fig. S5. HRTEM lattice fringe determinations for spinel-type $(Ni,V,Mn)_3O_{4-x}/Nb_2O_{5-y}$ nanoflowers on nickel foam.

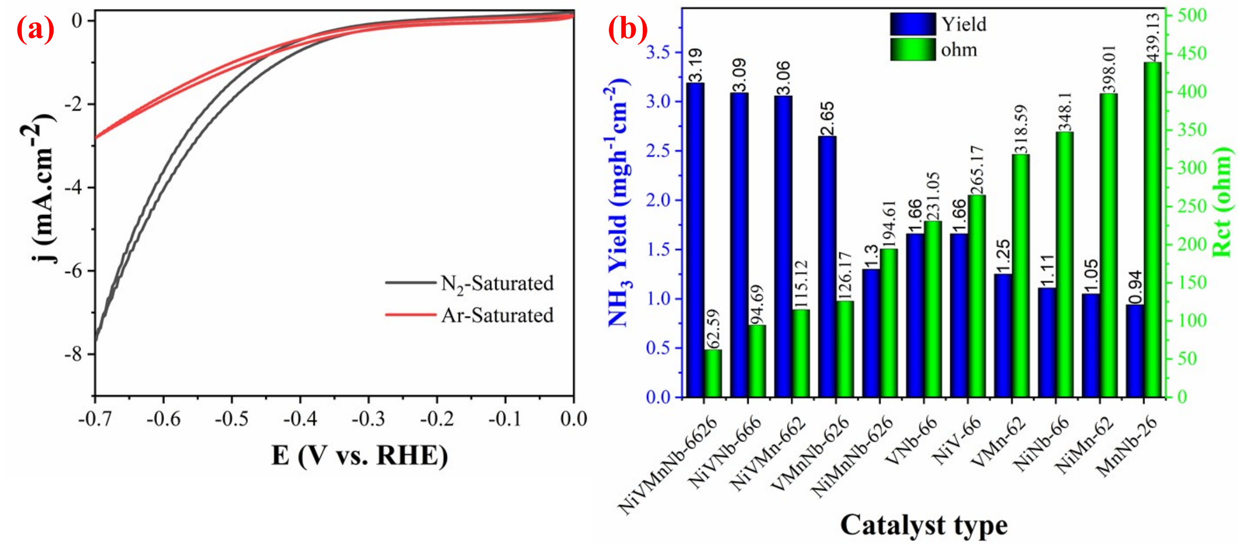

Fig. S6. (a) Cyclic voltammogram for quaternary NiVMnNb-6626 metal-oxide system in N_2 and Ar gas environments. (b) NH_3 Yield vs. Rct value of all catalyst types.

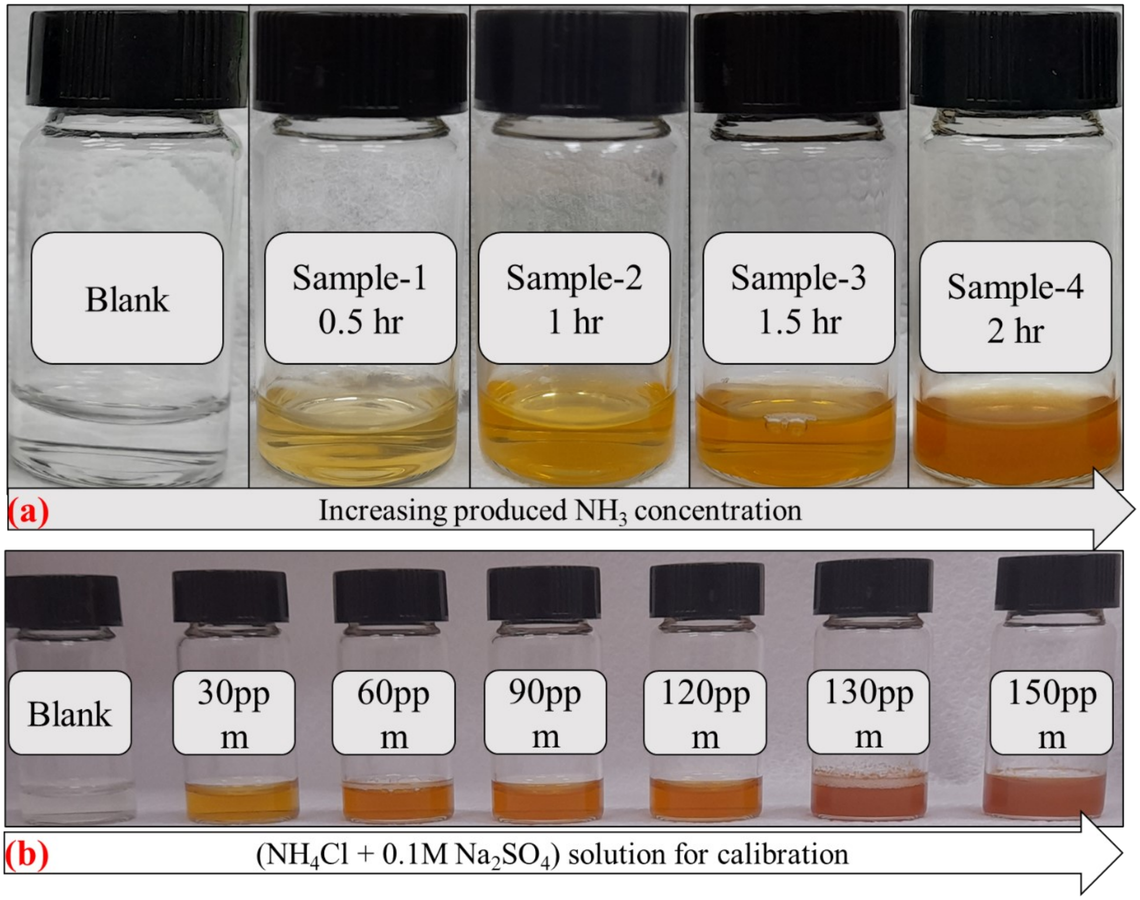

Fig. S7. NH_3 concentration (a) using spinel-type $(Ni,V,Mn)_3O_{4-x}/Nb_2O_{5-y}$ nanoflower quaternary metal-oxide system in N_2 environments for 2 hr, (b) the corresponding NH_4Cl + 0.1M Na_2SO_4 solution as a standard solution for calibration.

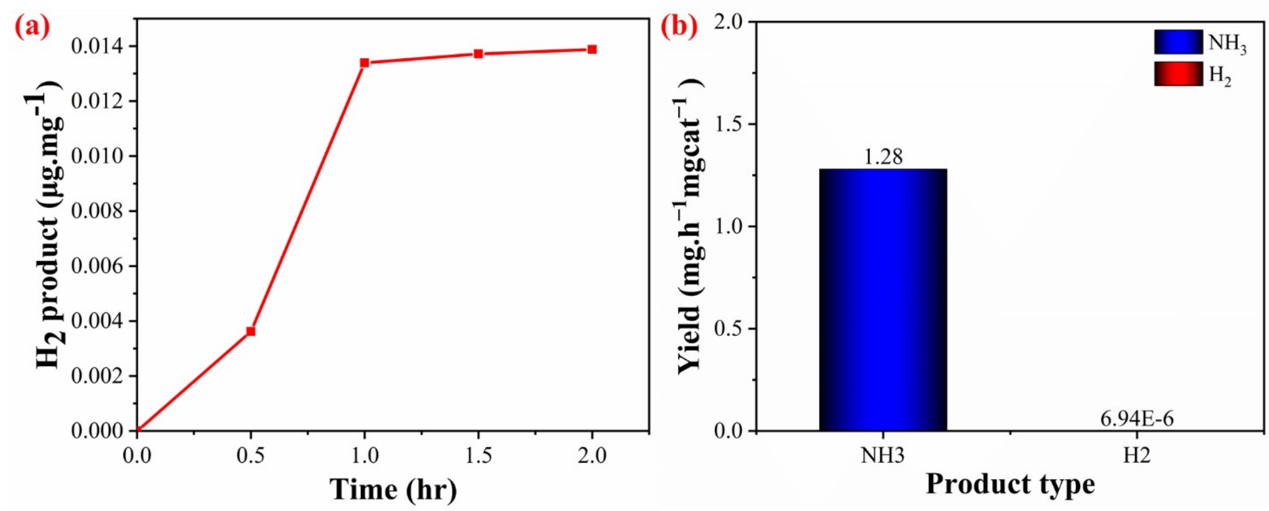

Fig. S8. a) Hydrogen concentration vs. reaction time b) NH_3 yield vs. H_2 production by spinel-type $(Ni,V,Mn)_3O_{4-x}/Nb_2O_{5-y}$ nanoflower quaternary metal-oxide system at the potential of -0.5 V vs. RHE in N_2 environments.

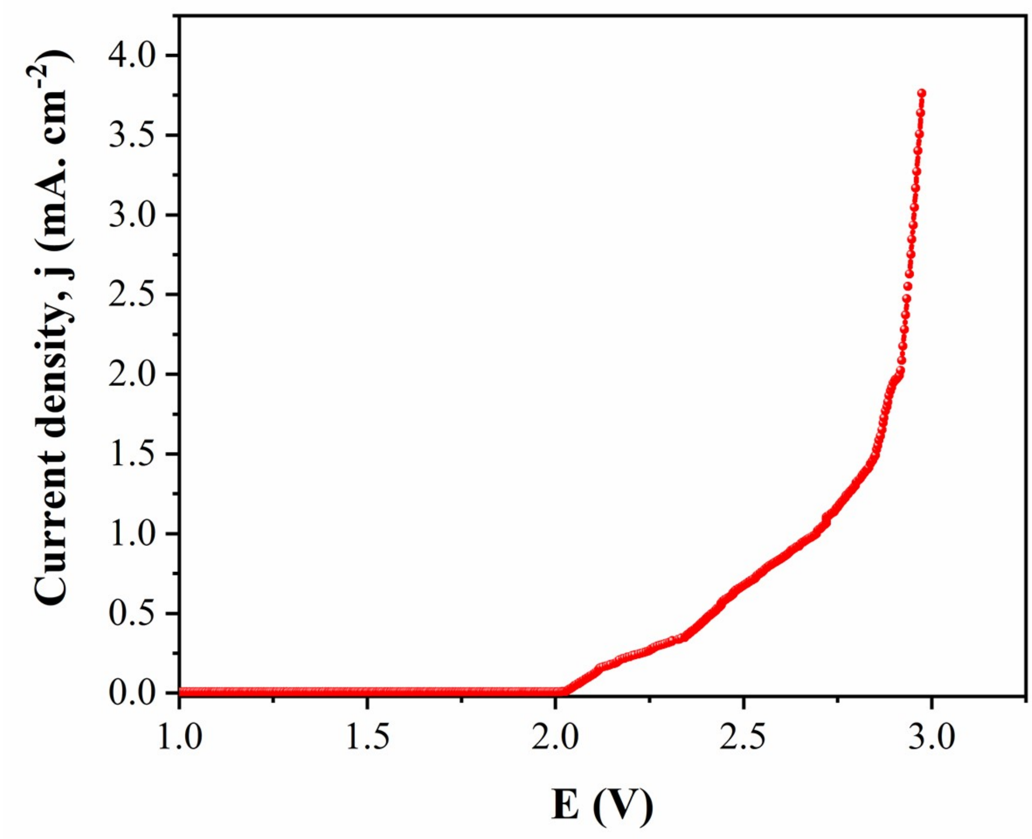

Fig. S9. LSV curve for a full cell with two-electrode system in a Na_2SO_4 electrolyte solution.

Table S1. Synthesized materials system naming and their sample size with mass loading

No.	Catalyst type	Ratio (in mmol)	Labeling	Weight (mg)	Sample size (cm^2)
1	NiVMnNb	6:6:2:6	NiVMnNb-6626	5	1x2
2	NiVNb	6:6:6	NiVNb-666	5	1x2
3	NiVMn	6:6:2	NiVMn-662	4.98	1x2
4	VMnNb	6:2:6	VMnNb-626	4.76	1x2
5	NiMnNb	6:2:6	NiMnNb-626	4.89	1x2
6	NiV	6:6	NiV-66	4.97	1x2
7	VNb	6:6	VNb-66	4.81	1x2
8	VMn	6:2	VMn-62	4.79	1x2
9	NiNb	6:6	NiNb-66	4.99	1x2
10	NiMn	6:2	NiMn-62	4.51	1x2
11	MnNb	6:2	MnNb-26	4.36	1x2

Note: During catalyst labeling, the elemental symbols indicate precursor metal type, and the number shows the ratio (in mmol) used during mixing.

Table S2. XPS compositional analysis of the NiVMnNb-6626 oxide system grown on Ni foam

Element	Ni	V	Mn	Nb	O
at.%	30.54	14.52	10.39	10.41	34.14

Table S3. XPS compositional analysis of NiVMnNb-6626 through the deconvoluted peak fitting to extract each element peak area to evaluate the valence state proportion

Element	Ni (%)	V (%)		Mn (%)		Nb (%)		O (%)	
	Ni^{+2}	V^{3+}	V^{4+}	Mn^{2+}	Mn^{3+}	Nb^{4+}	Nb^{5+}	O_L	O_V
at.%		60.3	39.7	36.8	63.2	82.3	17.7	81.9	18.1
Ratio	30.539	8.76	5.76	3.83	6.56	8.56	1.85	28.0	6.16

Table S4. HRSEM-EDS compositional analysis of NiVMnNb-6626 metal-oxide system.

Elements	Ni	V	Mn	Nb	O
at. %	26.57	16.22	1.63	0.34	55.24

Table S5. Charge transfer resistance of the Nyquist plot from EIS data

Electrocatalyst	NiVMnNb-6626	NiVNb-666	NiVMn-662	VMnNb-626	NiMnNb-626	NiV-66	VNb-66	VMn-62	NiNb-66	NiMn-62	MnNb-26
Rct	62.59	94.69	115.12	126.17	194.61	231.05	265.17	318.59	348.1	398.01	439.13

Table S6. Comparison of NH_3 yield and Faradic efficiency (FE) of the reported electrocatalysts with good performance

Catalyst	Electrolyte	NH_3 Yield	Catalyst amount	FE%	Ref.
Spinel-type $MnNi_{0.5}V_{1.5}O_4$/ Nb_2O_5 nanoflower	0.1 M Na_2SO_4	3.188 $mg.h^{-1}cm^{-2}$ 1.27 $mg.h^{-1}mg_{cat}^{-1}$	5 mg 2 cm^2	22.6	This work
VO_2	0.1 M Na_2SO_4	14.85 $\mu gh^{-1}mg^{-1}{}_{cat}$	0.2mg.cm^{-2}	3.97	1
VNiON	0.05 M Na_2SO_4	6.78 µg/h.cm^2	2 cm^2	5.57	2
Ni(NPs)@V_4C_3Tx	0.1 M KOH	21.29 $mg.h^{-1}mg_{cat}^{-1}$	0.16 mg.cm^{-2}	14.86	3
NbO_2	0.05 m H_2SO_4	11.6 $\mu gh^{-1}mg^{-1}{}_{cat}$	1 mg.cm^{-2}	32	4
Nb_2O_5	0.1 M HCl	43.6 $mg.h^{-1}mg_{cat}^{-1}$	0.1 mg	9.26	5
Ni_2GeO_4	0.1 M KOH	3.06 µg h^{-1} cm^{-2}	-	3.57	6
$LiMn_2O_4$	0.1 M HCl	15.83 µg h^{-1} mg_{cat}^{-1} 3.17 µg/h.cm^2	0.2 mg 1 cm^2	7.44	7
CoVP@NiFeV-LDHs HHNTs	0.05 M H_2SO_4	1.6×10^{-6} $mol.h^{-1}cm^{-2}$	1 mg 1 cm^2	13.8	8
N-C@NiO/GP	0.1 M HCl	14.022 µg h^{-1} mg_{cat}^{-1}	0.5 mg.cm^{-2}	30.43	9
Bi–K^+ pair	0.5 M K_2SO_4	200 mmol g^{-1} h^{-1} 884 µg cm^{-2} h^{-1}	94 µg cm^{-2}	66	10
SA-Ag/NC	0.1 M HCl	270.9 µg h^{-1} mg_{cat}^{-1} 54.2 µg/h.cm^2	0.2 mg 1 cm^2	21.90	11
Rh_2Sb	0.5 M Na_2SO_4	228.85 µg h^{-1} $mg^{-1}{}_{\mathbf{Rh}}$ 23.35 µg /h.cm^2	20 µg Rh 0.196 cm^2	6.10	12

Rh-Se NCs/C	0.1 M HCl	175.6 mg h^{-1} $g^{-1}_{\mathbf{Rh}}$ 17.92 μg/h.cm^2	0.02 mg 0.196 cm^2	13.3	13
Ru SAs/N-C	0.05 M H_2SO_4	120.9 μg h^{-1} mg_{cat}^{-1} 30.84 μg /h.cm^2	0.255mg.cm^{-2}	29.6	14
Au/C_3N_4	0.005 M H_2SO_4	1350 μg h^{-1} $mg_{\mathbf{Au}}^{-1}$ 30 μg h^{-1}.cm^2	0.5 cm^2	11.1	15
Pt SAs/WO_3	0.1 M K_2SO_4	342.4 μg h^{-1} $mg^{-1}_{\mathbf{Pt}}$ 10.27 μg/h.cm^2	0.03 mg 1 cm^2	31.1	16
FePc/C	0.1 M Na_2SO_4	137.95 μg $h^{-1}mg^{-1}_{\mathbf{FePc}}$ 137.95 μg /h.cm^2	0.25 mg 0.25 cm^2	10.5	17
GDY/Co_2N	0.1 M HCl	219.72 μg h^{-1} mg_{cat}^{-1}	6 cm^2	58.60	18
Pt/TiO_2	0.1 M NaOH	182 μg h^{-1} $mg_{cat.}^{-1}$ 182 μg h^{-1} cm^{-2}	1 cm^2	1.57	19

References

1. R. Zhang, H. Guo, L. Yang, Y. Wang, Z. Niu, H. Huang, H. Chen, L. Xia, T. Li, X. Shi, X. Sun, B. Li and Q. Liu, *ChemElectroChem*, 2019, **6**, 1014-1018.
2. B. Chang, L. Deng, S. Wang, D. Shi, Z. Ai, H. Jiang, Y. Shao, L. Zhang, J. Shen, Y. Wu and X. Hao, *J. Mater. Chem. A*, 2020, **8**, 91-96.
3. C.-F. Du, L. Yang, K. Tang, W. Fang, X. Zhao, Q. Liang, X. Liu, H. Yu, W. Qi and Q. Yan, *Mater Chem Front*, 2021, **5**, 2338-2346.
4. L. Huang, J. Wu, P. Han, A. M. Al-Enizi, T. M. Almutairi, L. Zhang and G. Zheng, *Small Methods*, 2019, **3**, 1800386.

5. J. Han, Z. Liu, Y. Ma, G. Cui, F. Xie, F. Wang, Y. Wu, S. Gao, Y. Xu and X. Sun, *Nano Energy*, 2018, **52**, 264-270.

6. D. Kim, S. Surendran, Y. Lim, H. Choi, J. Lim, J. Y. Kim, M.-K. Han and U. Sim, *Int. J. Energy Res.*, 2022, **46**, 4119-4129.

7. C. Li, J. Yu, L. Yang, J. Zhao, W. Kong, T. Wang, A. M. Asiri, Q. Li and X. Sun, *Inorg. Chem.*, 2019, **58**, 9597-9601.

8. M. Arif, G. Yasin, L. Luo, W. Ye, M. A. Mushtaq, X. Fang, X. Xiang, S. Ji and D. Yan, *Appl. Catal. B: Environ.*, 2020, **265**, 118559.

9. Y. Chen, B. Wu, B. Sun, N. Wang, W. Hu and S. Komarneni, *ACS Sustain. Chem. Eng.*, 2019, **7**, 18874-18883.

10. Y.-C. Hao, Y. Guo, L.-W. Chen, M. Shu, X.-Y. Wang, T.-A. Bu, W.-Y. Gao, N. Zhang, X. Su, X. Feng, J.-W. Zhou, B. Wang, C.-W. Hu, A.-X. Yin, R. Si, Y.-W. Zhang and C.-H. Yan, *Nat. Catal.*, 2019, **2**, 448-456.

11. Y. Chen, R. Guo, X. Peng, X. Wang, X. Liu, J. Ren, J. He, L. Zhuo, J. Sun and Y. Liu, *Acs Nano*, 2020, **14**, 6938-6946.

12. N. Zhang, L. Li, J. Wang, Z. Hu, Q. Shao, X. Xiao and X. Huang, *Angew. Chem., Int. Ed.*, 2020, **132**, 8143-8148.

13. C. Yang, B. Huang, S. Bai, Y. Feng, Q. Shao and X. Huang, *Adv. Mater.*, 2020, **32**, 2001267.

14. Z. Geng, Y. Liu, X. Kong, P. Li, K. Li, Z. Liu, J. Du, M. Shu, R. Si and J. Zeng, *Adv. Mater,*, 2018, **30**, 1803498.

15. X. Wang, W. Wang, M. Qiao, G. Wu, W. Chen, T. Yuan, Q. Xu, M. Chen, Y. Zhang, X. Wang, J. Wang, J. Ge, X. Hong, Y. Li, Y. Wu and Y. Li, *Science Bulletin*, 2018, **63**, 1246-1253.

16. R. Hao, W. Sun, Q. Liu, X. Liu, J. Chen, X. Lv, W. Li, Y. p. Liu and Z. Shen, *Small*, 2020, **16**, 2000015.

17. C. He, Z.-Y. Wu, L. Zhao, M. Ming, Y. Zhang, Y. Yi and J.-S. Hu, *ACS Catal.*, 2019, **9**, 7311-7317.

18. Y. Fang, Y. Xue, Y. Li, H. Yu, L. Hui, Y. Liu, C. Xing, C. Zhang, D. Zhang, Z. Wang, X. Chen, Y. Gao, B. Huang and Y. Li, *Angew. Chem. Int. Ed.*, 2020, **59**, 13021-13027.

19. J. L. Lv, Z. F. Tian, K. Dai, Y. X. Ye and C. H. Liang, *J. Colloid Interf. Sci.*, 2019, **553**, 126-135.